Chemical Engineering Journal 160 (2010) 13–19

Contents lists available at ScienceDirect

Chemical Engineering Journal

journal homepage: www.elsevier.com/locate/cej

Synthesis, characterization, and promoter effect of Cu-Zn/γ-Al_2O_3 catalysts on NO reduction with CO

Hui-Hsin Tseng[a,b,*], Hsiao-Yi Lin[a,b], Yu-Feng Kuo[a,b], Yi-Ting Su[a,b]

[a] School of Occupational Safety and Health, Chung Shan Medical University, Taichung 402, Taiwan, ROC
[b] Department of Occupational Medicine, Chung Shan Medical University Hospital, Taichung 402, Taiwan, ROC

ARTICLE INFO

Article history:
Received 2 September 2009
Received in revised form 11 February 2010
Accepted 20 February 2010

Keywords:
Polyol method
Bimetallic catalyst
NO reduction
CO oxidation
Promoter

ABSTRACT

The role of the Zn promoter and the preparation route in the catalytic properties of Cu-Zn/γ-Al_2O_3 catalysts towards NO reduction with CO were investigated in this study. The catalysts were prepared by chemical reduction of the corresponding metal species ($Cu(NO_3)_2\cdot2.5H_2O$ and $Zn(NO_3)_2\cdot6H_2O$) by a liquid polyol solution. The nano-bimetallic catalysts were obtained through this method, in which heterogeneous nucleation by seeding the reactive medium with foreign nuclei, Cu, was synthesized by the addition of an easier reductive metallic precursor to replace the homogeneous nucleation. Several samples were prepared with a variation in the reduction temperature, reduction time, Cu/Zn atomic ratio, and Cu and/or Zn loading weight in the catalysts. The morphology and surface chemical structure of the samples were assessed by transmission electron microscopy (TEM), BET surface area measurements, and X-ray photoelectron spectroscopy (XPS). Based on TEM evidence, the Cu-Zn/γ-Al_2O_3 catalysts were found to be composed of a spherical Cu-Zn nanoparticle, and the particle size decreased with the addition of Zn. XPS was used to study the different chemical states of the Zn-promoted Cu/γ-Al_2O_3, which indicated that the concentration of the reduced Cu species was related to the addition of Zn, thus increasing the NO conversion. The results obtained suggest that the use of Zn as a promoter and the polyol method as a preparation route played important roles in the properties of the catalysts, the Cu particle size, the reduction/oxidation efficiency of Cu/Zn, and the catalytic properties of NO reduction with CO.

© 2010 Published by Elsevier B.V.

1. Introduction

The selective catalytic reduction (SCR) of NO in the presence of oxygen with hydrocarbons [1–5] has been considered as a promising method for NO reduction due to its significant environmental impact. Among the different catalysts and active phase formulations that have been proposed for this reaction, Cu-based transition metal catalysts have been widely known for their SCR-CxHy reaction ever since Bethke et al. [2] found that Cu/γ-Al_2O_3 is highly active for the reduction of NO with C_3H_6 at a temperature of 315 °C. For this reaction, the activity is generally proportional to the Cu surface area, the dispersion, and the concentration of the oxidation state of Cu, Cu_2O, and CuO. Pillai and Deevi [6,7] also indicated that the rate-determining step for this reaction is related to in the oxidation state of Cu.

From a theoretical standpoint, the oxidation state of Cu-based catalysts can be modified through the multiple functions of the promoters or via the different preparation routes. For the former, various oxides and their mixtures have been used as a promoter for Cu, mostly ZnO and CeO_2 [8–10]. ZnO is known to improve both the dispersion of Cu and the reducibility of CuO, which have been cited as the possible reasons for the activity of Cu/ZnO catalysts if a Cu redox step occurs in the mechanism. However, it is also possible that improved adsorption can cause better activity. The adsorption properties of Cu/ZnO can affect activity because Zn can promote the formation of a linear or weakly bonded CO on the surface of Cu/ZnO [6]. Varying the synthesis routes also leads to changes in morphology, dispersion, and Cu species. Current preparation methods for SCR catalysts include the impregnation method [4,11], the ion exchange method [12], and the surfactant-templated method [8]. In the present work, the polyol method is used to synthesize Cu-Zn/γ-Al_2O_3, which was likewise employed for the preparation of nano-scaled photocatalysts in our previous study [13].

The polyol process is a kind of alcohol reduction method [14] known to be a chemical reduction agent-free method. In this process, a liquid polyol such as 1,2-ethanediol or 1,3-propanediol acts both as a solvent and as a mild reducing agent. The metal ions are mainly reduced by redox reaction between the metallic precursor and the solvent. The reaction mechanism has been investigated by Larcher and Patrice [15]. For the reduction of $Ni(OH)_2$ or $Co(OH)_2$

---

* Corresponding author at: School of Occupational Safety and Health, Chung Shan Medical University, Taichung 402, Taiwan, ROC. Tel.: +886 4 24730022x11823; fax: +886 4 23248194.
E-mail address: hhtseng@csmu.edu.tw (H.-H. Tseng).

1385-8947/$ – see front matter © 2010 Published by Elsevier B.V.
doi:10.1016/j.cej.2010.02.039

into metallic Ni or Co by ethylene glycol (EG), they found that the degradation of EG takes place in two steps. The first step is the dehydration of EG which gives rise to acetaldehyde, and the second is the duplicative oxidation of acetaldehyde with the formation of diacetyl [Eq. (1)]:

$$2CH_2OH\text{-}CH_2OH \rightarrow 2CH_3CHO + 2H_2O \tag{1}$$

This transformation was found to take place at the same time as the formation of metallic powder [Eq. (2)]:

$$2CH_3CHO + M(OH)_2 \rightarrow CH_3COCOCH_3 + 2H_2O + M^0\,(M = CoorNi) \tag{2}$$

In this process, nucleation and growth must be two completely separate steps to obtain monodisperse particles. It is well established that the concentration of the solute in the solution will affect the nucleation and growth rate, while the concentration reaches the critical supersaturation level when the spontaneous nucleation step begins. After the nucleation lowers the solute concentration below the self-nucleation level, the nucleation stage becomes short and is followed by the growth of the particles from the original nuclei for as long as the solute is slowly generated [16]. To decrease the solute generation rate and prevent the coagulation of particles during their growth stage, a dilute solution is used, or the pH of the solution is adjusted in order to increase the electrical repulsion between particles [17]. In some cases, protective agents such as PVP are also used to produce steric stabilization [18].

In the present study, the heterogeneous nucleation by seeding a reactive medium with a foreign nuclei, Cu, is synthesized by adding a more reductive metallic precursor $Cu(NO_3)_2$ to replace the homogeneous nucleation. Furthermore, to speed up the reduction of Cu(II) by EG, the reduction temperature needs to be increased, but it may exhibit a high degree of particle sintering. It is therefore necessary to restrain the temperature under appropriate conditions. To our knowledge, however, no reports on the polyol synthesis of Zn-promoted Cu/Al_2O_3 materials have been published to date.

As compared to the NH_3 reducing agent, CO was found to have lower reactivity towards NO [19–21] under low reaction temperature. In this paper, a series of nanosized Cu/Zn catalysts with different oxidation states was prepared by a polyol method under various conditions such as reduction temperature, reduction time, and Cu/Zn atomic ratio. Their catalytic performance towards NO reduction by CO was also investigated.

2. Experimental

2.1. Materials

Alumina (γ-Al_2O_3) supplied by Alfa-Aesar was used as the catalyst support throughout this work. Its main physical data are as follows: Brunauer–Emmett–Teller (BET) surface area (S_{BET}) 362.3 m^2/g, average pore size around 76.98 Å, and purity above 98%. Copper nitrate [$Cu(NO_3)_2 \cdot 2.5H_2O$] (Aldrich) and zinc nitrate [$Zn(NO_3)_2 \cdot 6H_2O$] (Aldrich) were used as the precursors corresponding to each catalyst. EG was used to reduce the metallic ions. Polyvinylpyrrolidone (PVP) (Sigma–Aldrich, molecular weight = 10000 $g\,mol^{-1}$) was used as a nucleation-protective agent to avoid nanoparticle sintering and aggregation.

2.2. Catalyst preparation

The supported mono-metallic Cu and bimetallic Cu/Zn catalysts were prepared as follows. The proper amounts of the precursors corresponding to the desired Cu/γ-Al_2O_3 or Cu-Zn/γ-Al_2O_3 weight ratio (Cu metal loading: 3 wt.%, ratio of Zn/Cu = 0.3, 0.5, 0.75 and 1 in atomic ratio) and 0.5 g of PVP were completely dissolved in EG-γ-Al_2O_3 solution. The reduction of the metallic ion was then produced by heating the mixed polyol solution up to the desired temperature (50–170 °C) at a rate of 5 °C min^{-1}, and this was kept for 0–60 min to react. At the end of the reaction time, the solution was rapidly cooled to 0 °C through an ice bath. Following filtration and washing, the resulting product was dried at 105 °C overnight and calcined in air at 400 °C for 4 h to remove the carbonate and crystal water which remaining on the surface of catalysts. Henceforth, they are abbreviated to CuZnx/γ-Al_2O_3-Y-Z (X, Y, and Z denote the Zn/Cu atomic ratio, reaction temperature, and reaction time, respectively).

2.3. Catalyst characterization

After calcination, the samples were characterized by flame atomic absorption spectroscopy (FAAS), BET, transmission electron microscopy (TEM), and X-ray photoelectron spectroscopy (XPS). The metal content in the catalysts was determined by FAAS. Before measuring, the samples were dissolved in dilute HNO_3-HF mixed solution by microwave digestion. The textural properties of the samples were measured by N_2 sorption at −196 °C with a PMI Automated BET Sorptometer (201AEL). TEM measurements were carried out with a JEOL 100CXII operating at 200 kV. During the preparation, the suspension was deposited on a Cu grid coated with a porous carbon film. XPS measurements were carried out on a PHI 5000 VersaProbe/Scanning ESCA Microprobe (ULVAC-PHI). All binding energies were corrected using a C 1s photoelectron peak at 284.6 eV as reference. The full widths of the peak at half maximum were allowed to adjust in order to attain the best fitting.

2.4. Catalytic tests

The catalytic activity of Cu/γ-Al_2O_3 or the Cu-Zn/γ-Al_2O_3 catalysts for the CO-SCR process was carried out in a continuous flow system with a fixed bed quartz reactor (15 mm I.D.) at atmospheric pressure. The experimental equipment consists of three sections: the gas feeding system, the reactor, and the gas analyzer. The catalysts were loaded with the aid of quartz wool and heated to the desired reaction temperature using an electric heater with PID controllers. Based on the stoichiometry (λ) of CO-SCR reaction ($2NO + CO \rightarrow N_2 + CO_2 + 1/2O_2$), we defined the λ as the ration of [NO]/[CO] ([NO]: concentration of NO; [CO]: concentration of CO) and discussed the effect of λ ($\lambda = 1$ and 2) on the NO conversion. Reagent gas mixtures containing NO, CO, 6% of O_2, and He as balance gas were adjusted by mass flow controllers (Brooks, 5850E). The corrosion resistant flow controllers were purged with high purity He between experiments. The total flow rate was 650 ml min^{-1}, which could be converted to a GHSV of $2.4 \times 10^4\,h^{-1}$, and the use of support particles size with a diameter range of 125–177 μm indicated that the mass and heat transfer limitations could be considered negligible by the calculation of effectiveness factors in our experimental conditions. Prior to the catalytic reaction, the catalysts were heated at the proper temperature in a He flow for 2 h. The catalytic activity was examined over a range of temperature (200–250 °C). After reaching the reaction temperature, the He gas flow was switched to the reactant feed gas flow. In all cases, the reaction was continued until the outlet stream concentration changed by less than 2%, at which time steady state conditions were assumed.

Concentrations of CO, CO_2, and NO were continuously measured by an online non-dispersive infrared gas analyzer (HORIBA PG-250A). The catalytic activity was evaluated in terms of NO conversion to N_2 and CO conversion to CO_2. The formation of NO_2 and N_2O analyzed by gas chromatograph with a thermal conductivity detector was found to be negligible in the present work because the selectivity of NO to N_2 was higher than 98% in all experiments.

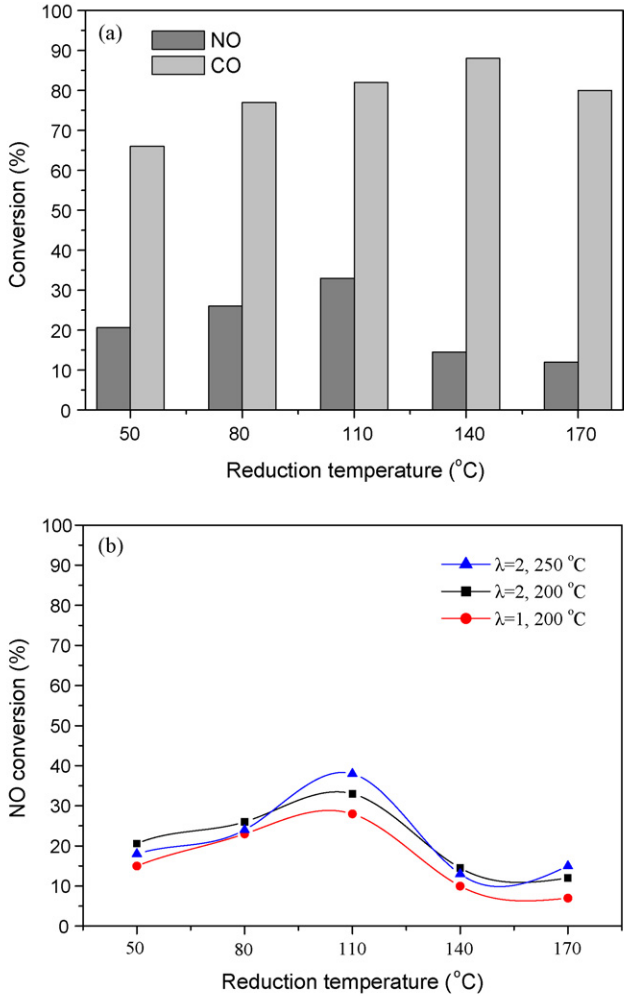

Fig. 1. Effect of reduction temperature on NO reduction by CO over Cu/γ-Al_2O_3-Y-10 catalysts. (Reaction conditions for (a): 400 ppm NO, 200 ppm CO, 6 vol% O_2, balance with He, total flow rate = 650 ml min^{-1}, GHSV = 24,375 h^{-1}, reaction temperature = 200 °C; for (b): 200/400 ppm NO, 200 ppm CO, 6 vol% O_2, balance with He, total flow rate = 650 ml min^{-1}, GHSV = 24,375 h^{-1}, reaction temperature = 200/250 °C).

3. Results and discussion

3.1. Effect of reduction temperature and reduction time

The activities of the Cu/γ-Al_2O_3-Y-10 catalysts prepared under different reduction temperatures for NO reduction by CO are shown in Fig. 1(a). The results indicate that the catalytic activity of Cu/γ-Al_2O_3-Y-10 catalysts prepared at either low or high temperature is relatively low, while the Cu/γ-Al_2O_3 catalysts prepared at suitable temperatures have a somewhat higher catalytic activity than the others. Specifically, the Cu/γ-Al_2O_3-140-10 catalyst can maintain the CO conversion at nearly 90% at 200 °C, and the Cu/γ-Al_2O_3-110-10 catalyst can maintain the NO conversion at nearly 33% at 200 °C respective of the oxygen inlets. With the increase in reduction temperature from 50 °C to 140 °C, the activities of the Cu/γ-Al_2O_3-Y-10 catalysts increase progressively, and the distinctions between the activities of Cu/γ-Al_2O_3-110-10 at different stoichiometric parameters λ (λ = [NO]/[CO]) and reaction temperatures become much evident [Fig. 1(b)]. Moreover, when the reduction temperature further increases beyond 140 °C, the activities of the Cu/γ-Al_2O_3-Y-10 catalysts decrease slowly.

The effect of reduction time on NO reduction with CO over the Cu/γ-Al_2O_3-140-Z catalysts is also investigated, and the results are shown in Fig. 2. It indicates that the catalytic activity of Cu/γ-Al_2O_3-140-Z prepared at a long reduction time has a higher conversion than that prepared at a short reduction time. With the increase in reduction time above 0 min, the activities of the Cu/γ-Al_2O_3-140-Z catalysts increase progressively, and the CO conversion increases from 77% over Cu/γ-Al_2O_3-140-0 to the highest conversion of 98% over Cu/γ-Al_2O_3-140-60. On the other hand, Cu/γ-Al_2O_3, with a suitable reduction time (40 min), has a somewhat higher activity for NO conversion than the others. To simultaneously remove CO and NO without high energy consumption, the CO and NO conversion of the catalysts should reach high conversion under a low reaction temperature. Therefore, Cu/γ-Al_2O_3-140-40 should be the most suitable catalyst for CO and NO conversion.

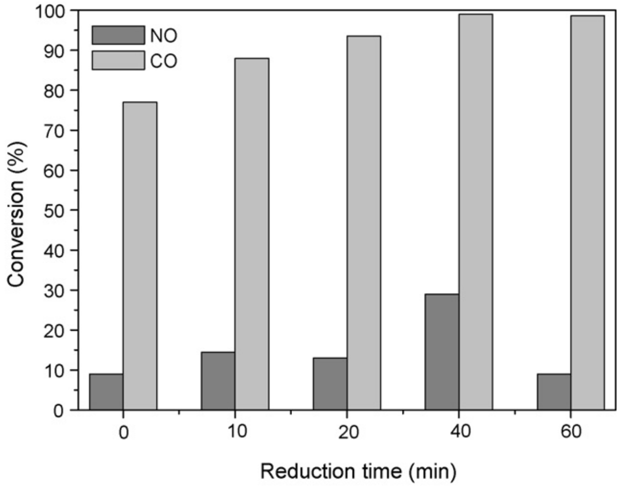

Fig. 2. Effect of reduction time on NO reduction with CO over Cu/γ-Al_2O_3-140-Z catalysts. (Reaction conditions: 400 ppm NO, 200 ppm CO, 6 vol% O_2, balance in He, total flow rate = 650 ml min^{-1}, GHSV = 24375 h^{-1}, reaction temperature = 200 °C).

3.2. Effect of the Zn promoter

The results obtained from the Zn-promoted Cu/γ-Al_2O_3-140-40 catalysts for NO reduction by CO with different Zn/Cu atomic ratios are given in Fig. 3. The promotion of Zn in the Cu/γ-Al_2O_3 catalysts provides a significant increase in the catalytic activity for NO and CO conversion, while the Zn-promoted Cu/γ-Al_2O_3 with 0.5 Zn atomic ratio has a somewhat higher catalytic activity towards NO conversion than the others, although it shows a slight decrease in CO conversion as compared to the 0.3 Zn atomic ratio. When

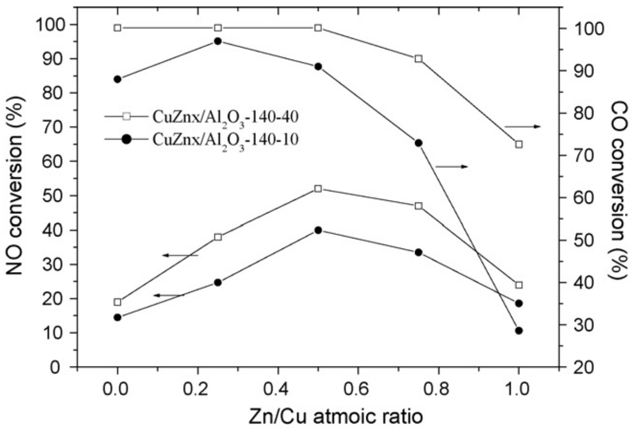

Fig. 3. Effect of Zn/Cu atomic ratio on NO reduction by CO over CuZnx/γ-Al_2O_3-140-Z catalysts. (Z = 10 and 40) (Reaction conditions: 400 ppm NO, 200 ppm CO, 6 vol% O_2, balance in He, total flow rate = 650 ml min^{-1}, GHSV = 24,375 h^{-1}, reaction temperature = 200 °C).

Table 1
BET surface area and experimental Cu/Zn content (wt.%) measured by FAAS for the supported samples.

Catalysts sample (Cu: 2.9 wt.%)	Cu (wt.%)	Zn (wt.%)	S_{BET} (m^2/g)	Catalysts sample (Cu: 2.9 wt.%)	Cu (wt.%)	Zn (wt.%)	S_{BET} (m^2/g)
Cu/γ-Al_2O_3-50-10	1.20	–	355.6	Cu/γ-Al_2O_3-140-10	1.86	–	324.5
Cu/γ-Al_2O_3-80-10	1.27	–	350.4	Cu/γ-Al_2O_3-140-40	1.96	–	320.2
Cu/γ-Al_2O_3-110-10	1.52	–	341.8	$CuZn_{0.25}$/γ-Al_2O_3-140-10	2.52	0.49	346.8
Cu/γ-Al_2O_3-170-10	2.36	–	309.8	$CuZn_{0.25}$/γ-Al_2O_3-140-40	2.67	0.62	343.6
Cu/γ-Al_2O_3-140-0	1.72	–	325.6	$CuZn_{0.5}$/γ-Al_2O_3-140-10	2.36	0.78	352.9
Cu/γ-Al_2O_3-140-20	1.88	–	324.8	$CuZn_{0.5}$/γ-Al_2O_3-140-40	2.58	0.97	350.6
Cu/γ-Al_2O_3-140-60	2.15	–	317.1	CuZn/γ-Al_2O_3-140-10	2.48	1.98	340.1
Raw aulmina	–	–	362.3				

the ratio is higher than 0.5, it is found that the catalytic activity decreases drastically. With a further increase in the Zn/Cu atomic ratio which is equivalent to 1, the negative impact of Zn on the catalytic activity of Cu/γ-Al_2O_3 increases substantially. As Chen and co-workers [22] reported, the presence of Zn increased appreciably the CO oxidation and NO reduction activity of the Cu catalysts. When Zn was incorporated into the catalysts, the reaction temperature could be decreased to reach the same conversion. In this study, the temperature at which about 95% of the CO conversion ($T_{>95\%}$) is attained at 200 °C, while the NO conversion is 52%. The addition of a 0.5 atom ratio (Zn/Cu) enhances the activity of the Cu/γ-Al_2O_3-140-40 catalysts, that is, a lower temperature at 200 °C of $T_{50\%}$ for NO reduction by CO.

3.3. Catalyst characterization

The elemental chemical analysis of the Cu/γ-Al_2O_3 catalysts prepared at different conditions is shown in Table 1. In the case of the samples with a lower reduction temperature, the results indicate that their Cu content is smaller than the initial Cu in the solution: 1.2 wt.% as opposed to 2.9 wt.% initially added. The poor deposition of metal onto the support was observed in a previous study. Sales et al. [23] and Bonet et al. [24] also found that silver metal ion was poorly deposited onto alumina, which was attributed to an incomplete reduction at a low temperature used for in situ deposition. Hence, significant amounts of Cu remained in the liquid phase as either unreduced or colloidal Cu. As the final reduction temperature used in this work for loading Cu onto alumina is increased, as shown in Table 1, the loading weight of Cu is also increased. At a reduction temperature of 50 °C, only about 41.3% of the initial metal loading was reduced and deposited on the surface of γ-Al_2O_3, while the temperature increased to 170 °C; the Cu loading weight achieved 81.3% reduction close to 2.36 wt.%. This might be attributed to the reduction temperature used in the polyol synthesis method, in which Cu could be reduced more completely under a higher reduction temperature above 170 °C. Table 1 also shows the effect of reduction time on the Cu loading weight. It was found that the amount of Cu loading on γ-Al_2O_3 increased slightly when the reduction time increased. Actually, the polyol method is based on a redox reaction between the metallic precursor and the solvent, and the reduction of metal ions is mainly governed by the difference between the oxidation potential of EG and the reduction potential of the Cu precursor at a given temperature [14]. Therefore, for the complete reduction of Cu ion, a higher temperature and longer deposition period would be required to decrease the oxidation potential of the solvent for a complete reduction of Cu ion.

The BET specific surface areas of raw support γ-Al_2O_3, as well as those loaded with Cu and/or Zn active sites, are listed in Table 1, indicating that the original surface area decreases as the Cu loading weight increases, especially those with high loading weight samples. These results can be explained by the aggregation of Cu particles at both the external and internal surfaces of the support, which may interfere with N_2 adsorption during the BET measurement. However, the surface area of the Zn-promoted Cu/γ-Al_2O_3 catalysts was increased upon the addition of Zn during the polyol synthesis process. Fig. 4 compares the pore volume and pore size distribution of Cu/γ-Al_2O_3, $CuZn_{0.25}$/γ-Al_2O_3, and $CuZn_{0.5}$/γ-Al_2O_3, which were prepared under the same conditions. The pore size distribution of the three catalysts appears to be not very different. However, the latter two catalysts show a higher pore volume than the unmodified catalyst, which contributes to their higher surface area (Table 1). Fig. 5 shows the TEM image of the resulting Cu/γ-Al_2O_3 catalyst prepared by the polyol method at 170 °C for 60 min. In this picture, it is observed that the Cu particles are loaded on the surface of the γ-Al_2O_3 support, and a large number of them are quasi-spherical nanoparticles with a size smaller than 5 nm in diameter. In accordance with the catalytic activity result, it is suggested that the active sites for CO and NO conversion should be more and should be highly dispersed on the surface of γ-Al_2O_3.

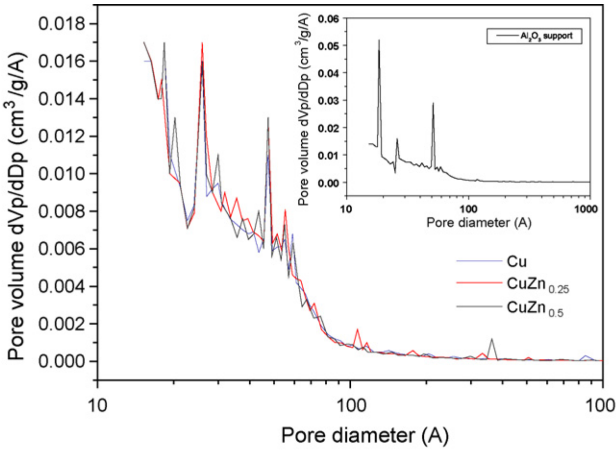

Fig. 4. Pore volume and pore size distribution of Cu/γ-Al_2O_3-140-40, $CuZn_{0.25}$/γ-Al_2O_3-140-40 and $CuZn_{0.5}$/γ-Al_2O_3-140-40 catalysts.

XPS measurement was further carried out to elucidate both the Cu structure and the chemical state of Zn. The binding energy values of the main peaks in the XPS spectra are summarized in Table 2, and the examination results on Cu 2p, O 1s, and Zn 2p

Table 2
Binding energy data Zn-promoted Cu/γ-Al_2O_3 catalysts prepared at different conditions.

Catalysts	Binding energy (eV)	
	Cu $2p_{3/2}$	Zn $2p_{3/2}$
Cu/γ-Al_2O_3-140-40	932.037	–
Cu/γ-Al_2O_3-140-10	932.600	–
$CuZn_{0.25}$/γ-Al_2O_3-140-40	932.230	1020.825
$CuZn_{0.5}$/γ-Al_2O_3-140-10	932.265	1021.381
$CuZn_{0.5}$/γ-Al_2O_3-140-40	932.311	1021.585
$CuZn_{0.75}$/γ-Al_2O_3-140-10	932.099	1021.305
$CuZn_{0.75}$/γ-Al_2O_3-140-40	932.151	1021.334

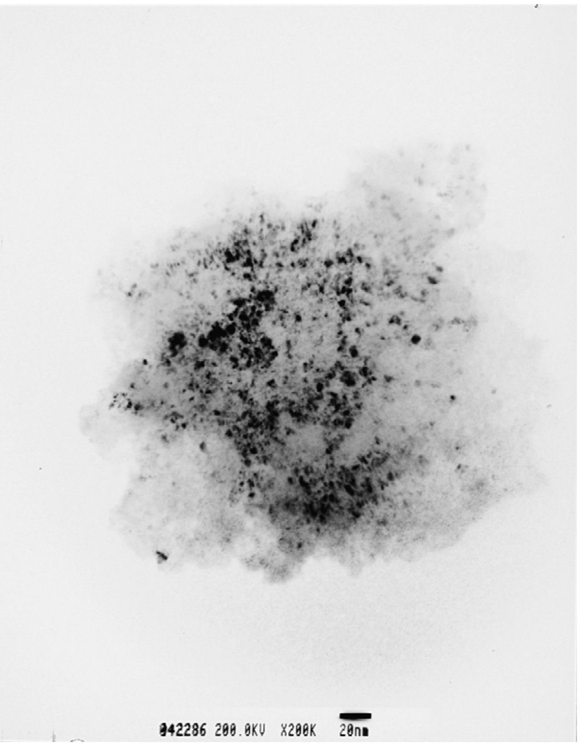

Fig. 5. TEM images of Cu/γ-Al_2O_3-170-60 catalysts prepared by polyol method.

XPS spectra are shown in Fig. 6(a)–(c). In Fig. 6(b), two distinctive XPS spectra of Cu $2p_{3/2}$ and Cu $2p_{1/2}$ (shake-up peak) are observed, and for the Cu/γ-Al_2O_3-140-10 sample, the binding energy was at 932.2 eV and 952.2 eV, respectively (see Table 2). Previous studies have shown the reference spectra of Cu particles, Cu metallic (Cu^0), monovalent Cu (Cu_2O), and divalent (CuO) to identify the Cu state [4,25,26]. The Cu 2p binding energies of Cu^0 were found to be 932.4 eV and 952.2 eV, respectively. However, the binding energies of Cu_2O were 0.4 eV and 0.6 eV over those for Cu^0 at 932.8 eV and 952.8 eV, respectively. For CuO, the binding energies were also only 1.0 eV over those for Cu_2O at 933.8 eV and 953.8 eV, respectively. Therefore, due to the similarity in binding energy value and peak shape, the chemical states of Cu^+ and Cu^0 are difficult to distinguish in the binding energy of Cu $2p_{3/2}$ [27]. As a result, the shake-up lines, the characterization of Cu^+ and Cu^{2+}, were used to identify them. According to the position and shape of the peaks, the Cu on the surface of γ-Al_2O_3 may exist in multiple-oxidation states, but Cu^+ is the primary species. In Zn-promoted Cu/γ-Al_2O_3, on the other hand, the peak shifted to a higher binding energy side. It was reported that the core-level binding energy of Cu significantly depended on the particle size of CuO and that the binding energy value of Cu $2p_{3/2}$ increased with the decrease in particle size of CuO supported on γ-Al_2O_3 [28]. Therefore, the binding energy shift towards a higher value with the promotion of Zn can be explained by the particle-size-induced effect. In other words, the addition of the Zn promoter helps to spatially separate or disperse the Cu particles phase on the γ-Al_2O_3 surface. However, the Cu $2p_{3/2}$ binding energy of the samples with a Zn/Cu ratio higher than 0.5 was slightly decreased from 934.4 eV to 933.2 eV. The most plausible explanation for the binding energy shift is the increase in electron density around Cu in the Zn-promoted Cu/γ-Al_2O_3 as a result of the electron donation from the promoter Zn. Due to the Fermi level of Cu being lower than that of Zn, the conduction band electron of Zn may transfer to the Cu species, resulting in an increase in the outer electron cloud density of the Cu ions.

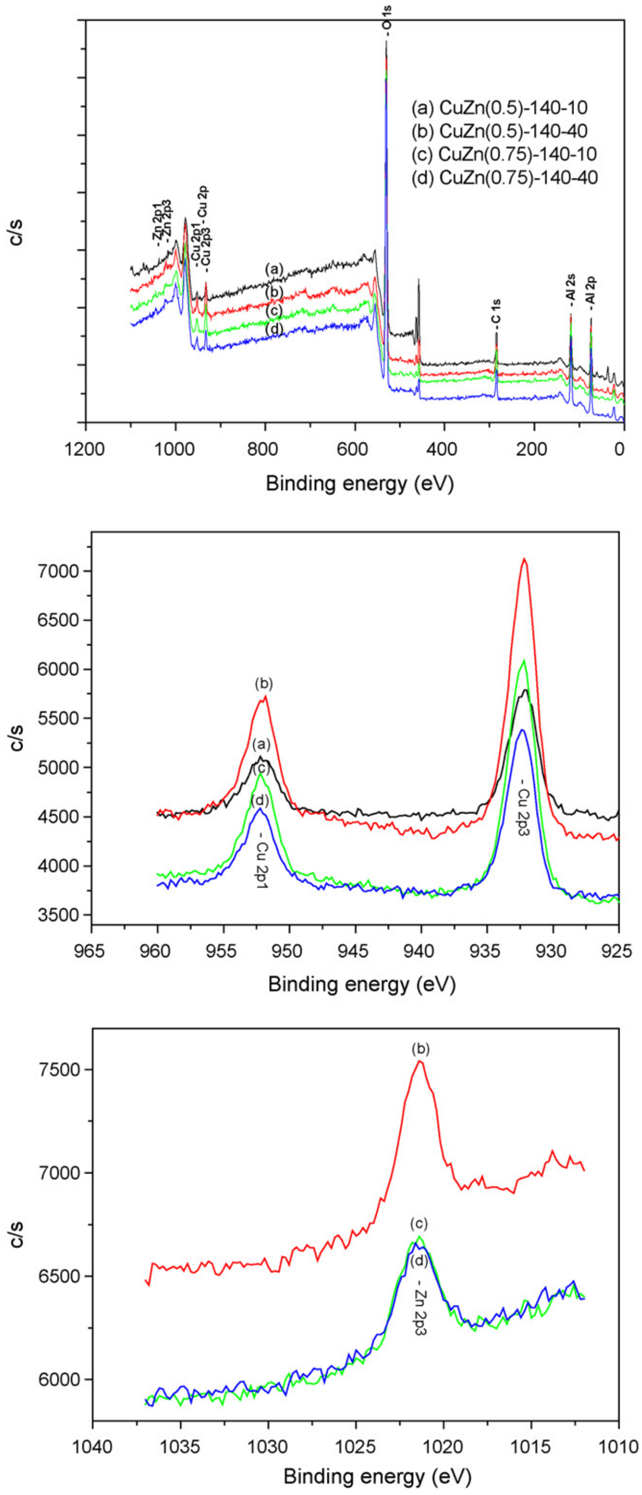

Fig. 6. (a) Survey of XPS spectra, (b) high-resolution Cu 2p XPS spectra and (c) high-resolution Zn 2p3 XPS spectra of bimetallic CuZn(X)/γ-Al_2O_3 catalysts (X = 0.5 and 0.75).

The Zn $2p_{3/2}$ XPS spectra of the Zn-promoted Cu/γ-Al_2O_3 catalysts are depicted in Fig. 6(c). One component, 1020.825 eV, observed in the spectrum can be assigned to the Zn^{2+} species through a comparison with the data reported in the literature [6]. Table 3 presents the composition of the CuZnx/γ-Al_2O_3 catalysts for various Zn/Cu ratios. For 2.9 wt.% Cu loading, the bulk Zn/Cu molar ratio was calculated to be about 0.25, 0.5, 0.75, and 1. FAAS analysis gave a reasonable Zn/Cu ratio compared with the expected value

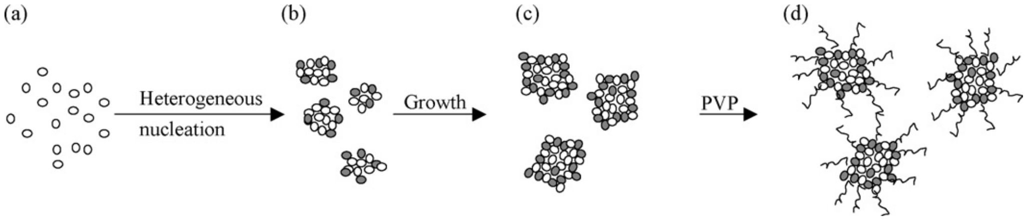

Fig. 7. Schematic representation of the formation process of highly dispersed Zn-promoted Cu/γ-Al_2O_3. (: copper,: zinc, and: surfactant).

for CuZnx/γ-Al_2O_3 catalysts, but the XPS Zn/Cu intensity ratio for all bimetal catalysts was markedly higher than the FAAS ratio. XPS can only detect the outermost surface (~10 nm) of a sample. This implies that the Zn concentrations on the surface were higher than those in the bulk medium for Cu/γ-Al_2O_3. The dispersion of Cu was enhanced by Zn reduction during the preparation process, which in turn reduced Zn as a dispersant.

The proposed mechanism for the formation of highly dispersed Zn-promoted Cu/γ-Al_2O_3 catalysts is illustrated in Fig. 7. At the initial stage of the nucleation process, many small amorphous Cu_2O and Cu could first be formed [Fig. 7(a)]. After this, heterogeneous nucleation and growth process by seeding the reactive medium with foreign nuclei, Cu, was occurred, and many small Zn was played as dispersing agents to prevent Cu_2O or Cu from aggregating [Fig. 7(c) and (d)]. On the other hand, in the process of crystal growth, the Gibbs free energies of the crystallites surface are usually very high, so the PVP molecules have the tendency to adsorb onto the surface to decrease the Gibbs free energies of these surfaces [29] [Fig. 7(d)].

3.4. Mechanism investigation

As stated above, the modification of Cu/γ-Al_2O_3 with Zn by the polyol method results in the significant improvement in CO and NO conversion activity as compared to the monometallic Cu/γ-Al_2O_3 catalyst. The NO reduction conversion over the $CuZn_{0.5}$/γ-Al_2O_3-140-40 catalyst is close to twice that of the Cu/γ-Al_2O_3-140-40 catalyst without losing CO oxidation conversion. Through physicochemcial characterizations as discussed above (including AA, BET, TEM, and XPS), the reaction mechanism as well as the role of Zn in the Zn-promoted Cu/γ-Al_2O_3 is discussed in this work. From the XPS results, a hint is given that the addition of the second metal Zn can improve the dispersion state of the Cu particles. During the polyol process, due to the standard reduction potential of Cu ($E^0 = 0.337\,V$) being higher than that of Zn ($E^0 = -0.763$), Cu may be reduced first and then covered by Zn, which helps separate the Cu particles to form a well-dispersed and relatively amorphous phase of Cu^0/Cu_2O. Pillai and Deevi [6,7] found that this amorphous or less crystalline Cu_2O phase can promote the formation of a more linearly (weakly) bonded CO on the catalyst surface and the evolution of active CuO species under the oxidizing conditions of the reaction. It could be deduced that CO was adsorbed on Zn^{2+} and then oxidized by neighboring Cu_2O, so the reduced Cu was produced. This phenomenon is evidence that metallic Cu^0 can be produced on the surface of the catalyst and then be oxidized by higher oxidization potential compounds such as NO. Epron et al. [30] found that metallic Cu can reduce nitrate according to a redox process, then CuO will be reduced with CO and/or Zn later. However, a higher amount of Zn increases the Cu electron density, hence resulting in the loss of reducibility despite improving the dispersion. From these results, we can conclude that the reducibility and propensity of variation in the oxidation states of Cu are critical to the activity of the catalyst, and this enhancement effect of activity over the Zn-promoted Cu/γ-Al_2O_3 bimetallic catalyst is due to the formation of the Zn active centers besides Cu. The simplified reaction mechanism scheme is presented in Fig. 8. With regard to the Zn-promoted catalyst, the role of Zn is to (i) disperse the Cu particles, (ii) enhance the redox properties of the CuO, and (iii) achieve a complete reduced state of the CuO phase at the interface.

Table 3
Results of FAAS and XPS analysis of Zn/Cu ratio on Cu-Znx/γ-Al_2O_3-140-10 catalysts.

Sample	Ratio by FAAS	Ratio by XPS
$CuZn_{0.25}$	0.19	0.18
$CuZn_{0.5}$	0.33	0.41
$CuZn_{0.75}$	0.62	0.68
CuZn	0.79	0.90

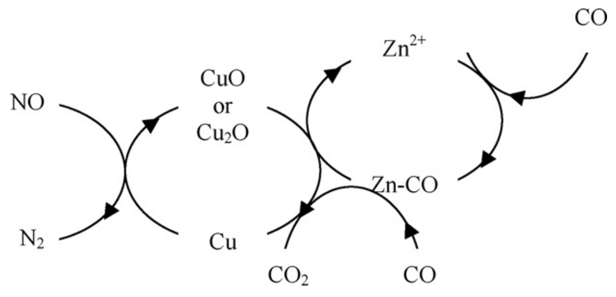

Fig. 8. The hypothetical reaction mechanism of catalytic reduction of NO with CO over Zn-promoted Cu/γ-Al_2O_3 catalysts.

4. Conclusion

In this study, we have altered a simple polyol process for the preparation of highly dispersed Cu/γ-Al_2O_3 with heterogeneous nucleation. This control route is easily and actively manipulated for NO reduction with CO. The XRD and XPS results show that the Zn-promoted catalysts possess highly dispersed surface Cu phases. For the Zu/Cu ratio lower than 0.5, the bimetallic catalysts possess a highly dispersed Cu phase with a high oxidation state. However, for the Zn/Cu ratio higher than 0.75, the electrons of Cu may be hidden by Zn which results in a lower activity for NO reduction even if the Cu is dispersed well.

References

[1] C. He, M. Paulus, W. Chu, J. Find, J.A. Nickl, K. Köhler, Selective catalytic reduction of NO by C_3H_8 over CoO_x/Al_2O_3: An investigation of structure–activity relationships, Catal. Today 131 (2008) 305.
[2] K.A. Bethke, M.C. Kung, B. Yang, M. Shah, D. Alt, C. Li, H.H. Kung, Metal oxide catalysts for lean NOx reduction, Catal. Today 26 (1995) 169.
[3] K.I. Shimizu, A. Satsuma, T. Hattori, Metal oxide catalysts for selective reduction of NO*x* by hydrocarbons: toward molecular basis for catalyst design, Catal. Surv. Japan 4 (2000) 115–123.
[4] T.W. Kim, M.W. Song, H.L. Koh, K.L. Kim, Surface properties and reactivity of Cu/γ-Al_2O_3 catalysts for NO reduction by C_3H_6: influences of calcination temperatures and additives, Appl. Catal. A 210 (2001) 35–44.
[5] N.A. Saidina Amin, C.M. Chong, SCR of NO with C_3H_6 in the presence of excess O_2 over Cu/Ag/CeO_2-ZrO_2 catalyst, Chem. Eng. J. 113 (2005) 13–25.
[6] U.R. Pillai, S. Deevi, Copper-zinc oxide and ceria promoted copper-zinc oxide as highly active catalysts for low temperature oxidation of carbon monoxide, Appl. Catal. B 65 (2006) 110–117.

[7] U.R. Pillai, S. Deevi, Room temperature oxidation of carbon monoxide over copper oxide catalyst, Appl. Catal. B 64 (2006) 146.

[8] M.F. Luo, J.M. Ma, J.Q. Lu, Y.P. Song, Y.J. Wang, High-surface area CuO–CeO_2 catalysts prepared by a surfactant-templated method for low-temperature CO oxidation, J. Catal. 246 (2007) 52–59.

[9] T. Shishido, Y. Yamamoto, H. Morioka, K. Takehira, Production of hydrogen from methanol over Cu/ZnO and Cu/ZnO/Al_2O_3 catalysts prepared by homogeneous precipitation: steam reforming and oxidative steam reforming, J. Mol. Catal. A 268 (2007) 185–194.

[10] H. Zou, X. Dong, W. Lin, Selective CO oxidation in hydrogen-rich gas over CuO/CeO_2 catalysts, Appl. Surf. Sci. 253 (2006) 2893–2898.

[11] A. Caballero, J.J. Morales, A.M. Cordon, J.P. Holgado, J.P. Espinos, A.R. Gonzalez-Elipe, An in situ XAS study of Cu/ZrO_2 catalysts under de-NO_x reaction conditions, J. Catal. 235 (2005) 295–301.

[12] J.W. Choung, In-Sik Nam, Role of cerium in promoting the stability of CuHM catalyst against HCl to reduce NO with NH_3, Appl. Catal. A 312 (2006) 165–174.

[13] H.H. Tseng, M.C. Wei, S.F. Hsiung, C.W. Chiou, Degradation of xylene vapor over Ni-doped TiO_2 photocatalysts prepared by polyol-mediated synthesis, Chem. Eng. J. 150 (2009) 160–167.

[14] D.W. Kim, J.M. Lee, C. Oh, D.S. Kim, S.G. Oh, A novel preparation route for platinum–polystyrene heterogeneous nanocomposite particles using alcohol-reduction method, J. Colloid Interf. Sci. 297 (2006) 365–369.

[15] D. Larcher, R. Patrice, Preparation of metallic powders and alloys in polyol media: a thermodynamic approach, J. Solid State Chem. 154 (2000) 405–411.

[16] G. Viau, F. Fiévet-Vincent, F. Fiévet, Nucleation and growth of bimetallic CoNi and FeNi monodisperse particles prepared in polyols, Solid State Ionics 84 (1996) 259–270.

[17] W. Li, W. Zhou, H. Li, Z. Zhou, B. Zhou, G. Sun, Q. Xin, Nano-stuctured Pt–Fe/C as cathode catalyst in direct methanol fuel cell, Electrochim. Acta 49 (2004) 1045–1055.

[18] M. Tsuji, P. Jiang, S. Hikino, S. Lim, R. Yano, S.M. Jang, S.H. Yoon, N. Ishigami, X. Tang, K. Sozana, N. Kamarudin, Toward to branched platinum nanoparticles by polyol reduction: a role of poly(vinylpyrrolidone) molecules, Colloids Surf. A: Physicochem. Eng. Aspects 317 (2008) 23–31.

[19] Y. Wang, A. Zhu, Y. Zhang, C.T. Au, X. Yang, C. Shi, Catalytic reduction of NO by CO over NiO/CeO_2 catalyst in stoichiometric NO/CO and NO/CO/O_2 reaction, Appl. Catal. B 81 (2008) 141–149.

[20] R.D. Monte, J. Kaspar, P. Fornasiero, M. Graziani, C. Pazée, G. Gubitosa, NO reduction by CO over Pd/$Ce_{0.6}Zr_{0.4}O_2$-Al_2O_3 catalysts: in situ FT-IR studies of NO and CO adsorption, Inorg. Chim. Acta 334 (2002) 318–326.

[21] Y. Wang, A. Zhu, Y. Zhang, C.T. Au, Z. Yang, C. Shi, Reduction of NO by CO on Cu/ZrO_2/Al_2O_3 catalysts: characterization and catalytic activities, Fuel 88 (2009) 1673–1679.

[22] C.S. Chem, J.H. You, J.H. Lin, C.R. Chen, K.M. Lin, The effect of a nickel promoter on the reducibility of a commercial Cu/ZnO/Al_2O_3 catalyst for CO oxidation, Catal. Commun. 9 (2008) 1230–1234.

[23] E.A. Sales, B. Benhamida, V. Caizergues, J.P. Lagier, F. Fiévet, F. Bozon-Verduraz, Alumina-supported Pd, Ag and Pd–Ag catalysts: preparation through the polyol process, characterization and reactivity in hexa-1,5-diene hydrogenation, Appl. Catal. A 172 (1998) 273–283.

[24] F. Bonet, C. Guery, D. Guyomard, R. Herrera Urbina, K. Tekaia-Elhsissen, J.-M. Tarascon, Electrochemical reduction of noble metal species in ethylene glycol at platinum and glassy carbon rotating disk electrodes, Solid State Ionics 126 (1999) 337–348.

[25] I.H. Tseng, J.C.S. Wu, H.Y. Chou, Effects of sol–gel procedures on the photocatalysis of Cu/TiO_2 in CO_2 photoreduction, J. Catal. 221 (2004) 432–440.

[26] W. Gao, J. Chen, X. Guan, R. Jin, F. Zhang, N. Guan, Catalytic reduction of nitrite ions in drinking water over Pd–Cu/TiO_2 bimetallic catalyst, Catal. Today 93 (2004) 333–339.

[27] Z. Wang, W. Wang, G. Lu, Studies on the active species and on dispersion of Cu in Cu/SiO_2 and Cu/Zn/SiO_2 for hydrogen production via methanol partial oxidation, Int. J. Hydrogen Energy 28 (2003) 151–158.

[28] H. Widjaja, K. Sekizawa, K. Eguchi, H. Arai, Oxidation of methane over Pd-supported catalysts, Catal. Today 35 (1997) 197–202.

[29] J. Zhu, Y. Wang, X. Wang, X. Yang, L. Lu, A convenient method for preparing shape-controlled nanocrystalline Cu_2O in a polyol or water/polyol system, Powder Technol. 181 (2008) 249–254.

[30] F. Epron, F. Gauthard, C. Pinéda, J. Barbier, Catalytic reduction of nitrate and nitrite on Pt–Cu/Al_2O_3 catalysts in aqueous solution: role of the interaction between copper and platinum in the reaction, J. Catal. 198 (2001) 309–318.